

## Effects of Alteration on Element Distributions in Archean Tholeiites from the Barberton Greenstone Belt, South Africa

Kent C. Condie<sup>1</sup>, M.J. Viljoen<sup>2</sup>, and E.J.D. Kable<sup>3</sup>

<sup>1</sup> Geoscience Department, New Mexico Institute of Mining and Technology,  
Socorro, New Mexico 87801, USA

<sup>2</sup> Johannesburg Consolidated Investment Company, Ltd., Randfontein, South Africa

<sup>3</sup> Nuclear Physics Research Unit, University of Witwatersrand, Johannesburg, South Africa

**Abstract.** Major and trace element and modal analyses are presented for unaltered, epidotized, and carbonated tholeiite flows from the Barberton greenstone belt. Au, As, Sb, Sr, Fe<sup>+3</sup>, Ca, Br, Ga, and U are enriched and H<sub>2</sub>O, Na, Mg, Fe<sup>+2</sup>, K, Rb, Ba, Si, Ti, P, Ni, Cs, Zn, Nb, Cu, Zr, and Co are depleted during epidotization. CO<sub>2</sub>, H<sub>2</sub>O, Fe<sup>+2</sup>, Ti, Zn, Y, Nb, Ga, Ta, and light REE are enriched and Na, Sr, Cr, Ba, Fe<sup>+3</sup>, Ca, Cs, Sb, Au, Mn, and U are depleted during carbonization-chloritization. The elements least affected by epidotization are Hf, Ta, Sc, Cr, Th, and REE; those least affected by carbonization-chloritization are Hf, Ni, Co, Zr, Th, and heavy REE. Both alteration processes can significantly change major element concentrations (and ratios) and hence caution should be used in distinguishing tholeiites from komatiites based on major elements alone. The amount of variation of many of the least mobile trace elements in the altered flows is approximately the same as allowed by magma model calculations. Hence, up to about 10% carbonization and 60% epidotization of tholeiite do not appreciably affect the interpretation of trace-element models for magma generation.

### Introduction

Many studies of the effects of low-temperature alteration on the composition of young basalts have appeared in the last several years (examples are Fey et al., 1974; Hart et al., 1974; Scott and Hajash, 1976). Results of these investigations indicate that both major and trace element concentrations can be significantly changed during alteration processes. One of the major problems associated with interpreting results from Archean greenstone volcanics is that of what the effect of alteration has been on the composition of the original rock.

To more fully understand the role of alteration, we herein report the results of a geochemical study of progressive epidotization and carbonization in tholeiites from the Barberton greenstone belt in South Africa. Although Archean

greenstones are metamorphosed to the greenschist (or amphibolite) facies, and hence it is not possible to obtain unmetamorphosed samples, many rocks show varying amounts of replacement by obvious secondary (syn- to post-metamorphic) minerals such as carbonate. The Barberton belt was selected for this investigation in that previous studies had shown that varying degrees of alteration exist in some rock units (Viljoen and Viljoen, 1962a-c). In order that an accurate representation of unaltered rock could be obtained, sampling was restricted to flow units where both unaltered and altered specimens could be taken from the same unit. Also, because existing studies of young pillowed basalt flows indicate wide and often nonsystematic element variations between pillow rims and cores (Scott and Hajash, 1976), only massive flows with rather uniform textures were sampled in this study. To allow comparison of element variabilities between unaltered and altered flows, samples were studied from both types of flows. One unaltered flow was sampled in the Hooggenoeg Formation in the Londozi River Valley about 10 km NNE of Steynsdorp. This massive flow, herein called the LR flow, is about 20 m thick and is exposed continuously along strike for over 1 km. Six samples were collected from this flow approximately equally spaced over the 1 km exposure. All samples were collected near the center of the flow. Two other flows which exhibit varying degrees of epidotization and carbonization were located in the Kromberg Formation in Komati Gorge (5 km NW of the LR flow): Several samples were collected from an epidotized flow (EP) and from a carbonated flow (CA) at this location. The epidotized suite was collected within an area of about 1 m<sup>2</sup> and the carbonated suite within an area of 10 m<sup>2</sup>. After petrographic examination, three samples from each flow showing the maximum range in secondary mineral content were selected for chemical analysis. One sample from each suite represented an unaltered sample of the flow.

### Analytical Methods

Most major elements were determined by X-ray fluorescence (XRF) in the Department of Geology, University of Witwatersrand, Johannesburg, South Africa. Fused discs were used employing a method similar to that described by Norrish and Hutton (1969). Ferrous Fe, H<sub>2</sub>O, and CO<sub>2</sub> were determined by conventional wet chemical methods (Shapiro and Brannock, 1956). Rb, Sr, Zr, Y, Cu, Zn, and Nb were determined by XRF using pressed powder pellets. Other trace elements were determined by INNA employing a 1 h thermal neutron irradiation and a 24 h epithermal irradiation at the Safari 1 Reactor, Pretoria, South Africa. The epithermal neutrons were obtained by irradiating samples in sealed cadmium cylinders. Details of the neutron activation methods are described in Steinnes (1971) and Rasmussen and Fesq (1973). Counting was done at NPRU at the University of Witwatersrand at 4, 7, and 30 days after irradiation. Corrections were made for the interference of the Ce<sup>141</sup> peak at 145 keV by Fe<sup>59</sup>. USGS rock standards were used to construct XRF major-element calibration curves. BCR-1 and an intralab basalt standard BLCR were used as standards for all trace element analyses. Errors for major elements are <3% and for trace elements ≤ 10%.

### Petrographic Features

In order to relate as closely as possible chemical differences in the samples to mineralogical differences, thin sections of all samples analyzed were described and modal analyses were made with an electric point-counter. Modes are given in Table 1 with the geochemical data. Actinolite and

Table 1. Major element and modal analyses of Archean tholeiites from the Barberton greenstone belt

|                                     | Londozi River (LR) Flow |       |       |        |       |       |           |        |                   | Carbonated (CA) Flow |        |       |        |        |                   |                   |        |       | Epidotized (EP) Flow |        |                   |                   |        |       |        |  |  |
|-------------------------------------|-------------------------|-------|-------|--------|-------|-------|-----------|--------|-------------------|----------------------|--------|-------|--------|--------|-------------------|-------------------|--------|-------|----------------------|--------|-------------------|-------------------|--------|-------|--------|--|--|
|                                     | 17                      | 18    | 19    | 20     | 21    | 22    | $\bar{X}$ | 4      | 3                 | 2                    | 7      | 8     | 9      | 4      | 3                 | 2                 | 7      | 8     | 9                    | 4      | 3                 | 2                 | 7      | 8     | 9      |  |  |
| SiO <sub>2</sub>                    | 51.0                    | 52.0  | 51.7  | 52.6   | 51.7  | 51.6  | 51.8      | 50.8   | 50.6              | 47.1                 | 51.3   | 50.5  | 46.6   | 50.8   | 50.6              | 47.1              | 51.3   | 50.5  | 46.6                 | 50.8   | 50.6              | 47.1              | 51.3   | 50.5  | 46.6   |  |  |
| TiO <sub>2</sub>                    | 1.04                    | 1.05  | 0.98  | 1.06   | 1.00  | 1.05  | 1.03      | 1.37   | 1.43              | 1.65                 | 0.90   | 0.81  | 0.73   | 1.37   | 1.43              | 1.65              | 0.90   | 0.81  | 0.73                 | 1.37   | 1.43              | 1.65              | 0.90   | 0.81  | 0.73   |  |  |
| Al <sub>2</sub> O <sub>3</sub>      | 9.73                    | 10.2  | 9.54  | 10.5   | 9.92  | 10.2  | 10.0      | 14.0   | 13.7              | 13.2                 | 14.8   | 15.1  | 15.5   | 14.0   | 13.7              | 13.2              | 14.8   | 15.1  | 15.5                 | 14.0   | 13.7              | 13.2              | 14.8   | 15.1  | 15.5   |  |  |
| Fe <sub>2</sub> O <sub>3</sub>      | 1.32                    | 1.24  | 1.31  | 1.32   | 1.45  | 1.31  | 1.33      | 3.45   | 1.74              | 1.81                 | 2.69   | 4.34  | 9.63   | 3.45   | 1.74              | 1.81              | 2.69   | 4.34  | 9.63                 | 3.45   | 1.74              | 1.81              | 2.69   | 4.34  | 9.63   |  |  |
| FeO                                 | 9.6                     | 9.3   | 9.7   | 9.3    | 9.4   | 9.3   | 9.4       | 9.9    | 10.7              | 13.1                 | 9.1    | 5.7   | 3.0    | 9.9    | 10.7              | 13.1              | 9.1    | 5.7   | 3.0                  | 9.9    | 10.7              | 13.1              | 9.1    | 5.7   | 3.0    |  |  |
| MnO                                 | 0.16                    | 0.17  | 0.16  | 0.12   | 0.17  | 0.13  | 0.15      | 0.19   | 0.13              | 0.15                 | 0.19   | 0.18  | 0.21   | 0.19   | 0.13              | 0.15              | 0.19   | 0.18  | 0.21                 | 0.19   | 0.13              | 0.15              | 0.19   | 0.18  | 0.21   |  |  |
| MgO                                 | 12.8                    | 11.7  | 12.5  | 11.2   | 11.9  | 11.2  | 11.9      | 5.93   | 5.42              | 6.05                 | 7.58   | 5.35  | 3.58   | 5.93   | 5.42              | 6.05              | 7.58   | 5.35  | 3.58                 | 5.93   | 5.42              | 6.05              | 7.58   | 5.35  | 3.58   |  |  |
| CaO                                 | 8.76                    | 8.38  | 8.50  | 8.63   | 8.34  | 8.74  | 8.56      | 8.93   | 5.97              | 4.55                 | 7.50   | 13.2  | 18.9   | 8.93   | 5.97              | 4.55              | 7.50   | 13.2  | 18.9                 | 8.93   | 5.97              | 4.55              | 7.50   | 13.2  | 18.9   |  |  |
| Na <sub>2</sub> O                   | 1.70                    | 1.60  | 1.29  | 1.49   | 1.29  | 1.76  | 1.52      | 2.57   | 2.59              | 1.11                 | 2.48   | 2.50  | 1.09   | 2.57   | 2.59              | 1.11              | 2.48   | 2.50  | 1.09                 | 2.57   | 2.59              | 1.11              | 2.48   | 2.50  | 1.09   |  |  |
| K <sub>2</sub> O                    | 0.37                    | 0.77  | 0.66  | 1.09   | 1.16  | 1.05  | 0.85      | 0.24   | 0.10              | 0.85                 | 0.59   | 0.60  | 0.19   | 0.24   | 0.10              | 0.85              | 0.59   | 0.60  | 0.19                 | 0.24   | 0.10              | 0.85              | 0.59   | 0.60  | 0.19   |  |  |
| P <sub>2</sub> O <sub>5</sub>       | 0.17                    | 0.12  | 0.11  | 0.11   | 0.12  | 0.11  | 0.12      | 0.14   | 0.15              | 0.16                 | 0.09   | 0.06  | 0.05   | 0.14   | 0.15              | 0.16              | 0.09   | 0.06  | 0.05                 | 0.14   | 0.15              | 0.16              | 0.09   | 0.06  | 0.05   |  |  |
| H <sub>2</sub> O                    | 3.1                     | 2.6   | 3.0   | 2.7    | 2.7   | 2.7   | 2.8       | 2.6    | 4.3               | 6.2                  | 3.1    | 1.5   | 0.7    | 2.6    | 4.3               | 6.2               | 3.1    | 1.5   | 0.7                  | 2.6    | 4.3               | 6.2               | 3.1    | 1.5   | 0.7    |  |  |
| CO <sub>2</sub>                     | 0.1                     | ≈0.1  | ≈0.1  | ≈0.1   | ≈0.1  | ≈0.1  | ≈0.1      | ≈0.1   | 3.3               | 4.2                  | ≈0.1   | 0.1   | ≈0.1   | ≈0.1   | 3.3               | 4.2               | ≈0.1   | 0.1   | ≈0.1                 | ≈0.1   | 3.3               | 4.2               | ≈0.1   | 0.1   | ≈0.1   |  |  |
| Total                               | 99.85                   | 99.59 | 99.55 | 100.22 | 99.25 | 99.25 | 99.46     | 100.22 | 100.13            | 100.22               | 100.42 | 99.94 | 100.18 | 100.22 | 100.13            | 100.22            | 100.42 | 99.94 | 100.18               | 100.22 | 100.13            | 100.22            | 100.42 | 99.94 | 100.18 |  |  |
| Fe <sub>2</sub> O <sub>3</sub> /FeO | 0.14                    | 0.13  | 0.14  | 0.14   | 0.15  | 0.14  | 0.14      | 0.35   | 0.16              | 0.14                 | 0.30   | 0.76  | 3.21   | 0.35   | 0.16              | 0.14              | 0.30   | 0.76  | 3.21                 | 0.35   | 0.16              | 0.14              | 0.30   | 0.76  | 3.21   |  |  |
| CaO/Al <sub>2</sub> O <sub>3</sub>  | 0.90                    | 0.82  | 0.89  | 0.82   | 0.84  | 0.86  | 0.86      | 0.64   | 0.44              | 0.34                 | 0.51   | 0.87  | 1.2    | 0.64   | 0.44              | 0.34              | 0.51   | 0.87  | 1.2                  | 0.64   | 0.44              | 0.34              | 0.51   | 0.87  | 1.2    |  |  |
| Actinolite                          | 67.9                    | 59.7  | 68.6  | 59.3   | 62.4  | 50.9  | 61.5      | 49.0   | 44.2 <sup>a</sup> | 46.0 <sup>a</sup>    | 46.5   | 36.8  | 25.2   | 49.0   | 44.2 <sup>a</sup> | 46.0 <sup>a</sup> | 46.5   | 36.8  | 25.2                 | 49.0   | 44.2 <sup>a</sup> | 46.0 <sup>a</sup> | 46.5   | 36.8  | 25.2   |  |  |
| Plagioclase                         | 17.5                    | 16.6  | 15.0  | 16.4   | 14.4  | 18.7  | 16.4      | 29.0   | 23.6              | 12.4                 | 38.2   | 29.9  | 12.2   | 29.0   | 23.6              | 12.4              | 38.2   | 29.9  | 12.2                 | 29.0   | 23.6              | 12.4              | 38.2   | 29.9  | 12.2   |  |  |
| Chlorite                            | 3.1                     | 5.2   | 3.3   | 6.1    | 4.0   | 4.3   | 4.3       | 8.2    | 18.4              | 24.2                 | 3.3    | 4.2   | 1.0    | 8.2    | 18.4              | 24.2              | 3.3    | 4.2   | 1.0                  | 8.2    | 18.4              | 24.2              | 3.3    | 4.2   | 1.0    |  |  |
| Epidote                             | 1.2                     | 7.3   | 4.4   | 3.6    | 3.1   | 6.5   | 4.4       | 9.0    | —                 | —                    | 6.9    | 23.6  | 58.5   | 9.0    | —                 | —                 | 6.9    | 23.6  | 58.5                 | 9.0    | —                 | —                 | 6.9    | 23.6  | 58.5   |  |  |
| Opaque <sup>b</sup>                 | 1.7                     | 2.7   | 2.4   | 0.9    | 2.2   | 4.5   | 2.4       | 1.0    | 2.1               | 3.7                  | 1.4    | 0.2   | 0.1    | 1.0    | 2.1               | 3.7               | 1.4    | 0.2   | 0.1                  | 1.0    | 2.1               | 3.7               | 1.4    | 0.2   | 0.1    |  |  |
| Quartz                              | tr                      | tr    | tr    | 0.5    | tr    | tr    | tr        | 0.9    | 2.1               | 1.5                  | 1.2    | 2.3   | 0.9    | 0.9    | 2.1               | 1.5               | 1.2    | 2.3   | 0.9                  | 0.9    | 2.1               | 1.5               | 1.2    | 2.3   | 0.9    |  |  |
| Clinopyroxene                       | 4.2                     | 2.3   | 1.2   | 3.3    | 3.5   | 4.8   | 3.2       | —      | —                 | —                    | —      | —     | —      | —      | —                 | —                 | —      | —     | —                    | —      | —                 | —                 | —      | —     | —      |  |  |
| Sphene                              | 1.2                     | tr    | —     | 0.3    | —     | 1.2   | 0.5       | 2.8    | 1.5               | 1.9                  | 2.4    | 2.1   | 1.9    | 2.8    | 1.5               | 1.9               | 2.4    | 2.1   | 1.9                  | 2.8    | 1.5               | 1.9               | 2.4    | 2.1   | 1.9    |  |  |
| Mica                                | 3.2                     | 6.2   | 5.1   | 9.6    | 10.4  | 9.1   | 7.3       | —      | —                 | —                    | —      | —     | —      | —      | —                 | —                 | —      | —     | —                    | —      | —                 | —                 | —      | —     | —      |  |  |
| Carbonate                           | tr                      | —     | —     | —      | —     | —     | —         | tr     | 7.9               | 9.0                  | —      | —     | —      | tr     | 7.9               | 9.0               | —      | —     | —                    | tr     | 7.9               | 9.0               | —      | —     | —      |  |  |

<sup>a</sup> Including fine-grained chlorite, sericite, and plagioclase<sup>b</sup> Principally limonite-goethite with minor magnetite, leucoxene, and sulfide

sodic plagioclase (oligoclase) are the two most abundant minerals in the LR flow and in the unaltered CA and EP flows (samples 4 and 7, respectively). The plagioclase is saussuritized, partially replaced with chlorite, and exhibits poorly developed twins. The existence of clinopyroxene in the LR flow was verified by electron-probe scans. The clinopyroxene occurs as cores in actinolite and appears to represent remnants of original pyroxene in the basalt. Sphene commonly shows skeletal crystal forms and cross-cuts other minerals suggesting late development. Although most of the opaque fraction appears to be limonite-goethite, reflected-light optical examination indicates the presence of minor, widely scattered, sulfide grains (chiefly pyrite) in most samples. Micas in the samples are extremely fine-grained.

In the EP sample suite, epidote increases in abundance up to about 60%. Textural relations clearly indicate that it replaces actinolite and plagioclase. In the CA suite, carbonate increases from trace amounts to about 10% and is paralleled by an increase in chlorite from 8 to 24%. Both minerals replace actinolite and plagioclase, and in some instances pseudomorphs of actinolite can be identified. Textures indicate that epidotization and carbonization-chloritization are post-metamorphic processes and hence should not be equated with deuteritic alteration, seawater interaction (halmyrolysis), or low-grade metamorphism. The fact that original subophitic textures in the flows are well-preserved as pseudomorphic outlines, attests furthermore to the absence of significant deformation during either low-grade metamorphism or later alteration.

### Flow Variability

Results of major and trace element analyses and modal analyses are given in Tables 1 and 2 together with pertinent element ratios. A comparison of hand specimen variability with intra-flow variability in the LR flow is summarized in Figure 1. Hand specimen variability is estimated from the analyses of three aliquots of sample 22. As is evident from the Figure, many elements have approximately the same variability in both the hand specimen and in the flow. Sb, Au, and As, however, are more variable by an order or magnitude in the flow than in the hand specimen. This may be due to the very irregular distribution of sulfides in the flow. Ni, Cr, Cs, Ga, Ba, and Rb are also somewhat more variable in the flow than in the hand specimen. In the case of Ba, Cs, and Rb, the large intraflow variability may be controlled by the variability in mica content (Table 1). It is clear from the results shown in Figure 2a that the variation in REE patterns in the hand specimen is approximately the same as in the flow. Care should be exercised in using those elements which exhibit relatively large intraflow variability in classifying or studying the origin of Archean volcanic rocks when only a few analyses are available.

Major-element variation in the LR flow roughly parallels controlling mineralogical variations (Table 1). There are only a few clearly defined relationships between trace-element distributions and mineralogy, however. Most obvious are the variations in Rb, K/Cs, K/Rb, and La/Yb which broadly parallel mica variations. Iron oxides and sulfides are relatively abundant in sample 22 as are As, Sb, and Au. Sample 9, which has a high transition-metal content, has the highest total amount of actinolite + clinopyroxene + epidote. It is of interest to see if any of the now well-documented chemical changes characteristic of low-temperature alteration (halmyrolysis) appear in the LR flow.  $\text{Fe}^{+3}$ ,  $\text{H}_2\text{O}$ , K, and Cs commonly increase with degree of alteration and a negative correlation exists between K and K/Rb, K/Cs, and K/Ba (Hart, 1969; Hart et al., 1974). None of these trends characterize the LR flow and in fact, a rough positive

**Table 2.** Trace element analyses of Archean tholeiites from the Barberton greenstone belt

|        | Londoz River (LR) Flow |      |      |      |      |      | Carbonated (CA) Flow |      |       |      |      |       | Epidotitized (EP) Flow |   |   |   |   |   |
|--------|------------------------|------|------|------|------|------|----------------------|------|-------|------|------|-------|------------------------|---|---|---|---|---|
|        | 17                     | 18   | 19   | 20   | 21   | 22   | $\bar{X}$            | 3    | 4     | 2    | 7    | 8     | 9                      | 3 | 4 | 2 | 7 | 8 |
| Sc     | 24                     | 23   | 25   | 22   | 24   | 23   | 24                   | 35   | 28    | 32   | 33   | 31    | 30                     |   |   |   |   |   |
| Cr     | 1200                   | 1190 | 1370 | 1090 | 1220 | 1150 | 1204                 | 150  | 63    | 63   | 68   | 77    | 68                     |   |   |   |   |   |
| Co     | 70                     | 71   | 79   | 69   | 71   | 69   | 72                   | 54   | 53    | 50   | 54   | 51    | 31                     |   |   |   |   |   |
| Ni     | 800                    | 680  | 830  | 650  | 840  | 710  | 750                  | 125  | 140   | 106  | 123  | 88    | 76                     |   |   |   |   |   |
| Cu     | 140                    | 146  | 149  | 164  | 100  | 133  | 139                  | 177  | 137   | 170  | 36   | 49    | 56                     |   |   |   |   |   |
| Zn     | 104                    | 86   | 108  | 88   | 97   | 96   | 96                   | 120  | 119   | 163  | 195  | 69    | 88                     |   |   |   |   |   |
| Sb     | 0.75                   | 0.66 | 0.85 | 0.77 | 0.80 | 1.7  | 0.92                 | 0.40 | 0.25  | 0.4  | 0.35 | 1.3   | 3.1                    |   |   |   |   |   |
| As     | 4.8                    | 1.0  | 1.5  | 0.76 | 2.5  | 6.4  | 2.8                  | 0.42 | 0.50  | 0.36 | ~0.1 | 1.5   | 0.63                   |   |   |   |   |   |
| Au     | 1.6                    | 1.1  | 0.86 | 7.1  | 2.9  | 4.5  | 3.0                  | 1.0  | 0.60  | 0.62 | 0.80 | 7.9   | 2.2                    |   |   |   |   |   |
| Ga     | 14                     | 10   | 12   | 12   | 8.1  | 12   | 11                   | 13   | 18    | 14   | 11   | 13    | 17                     |   |   |   |   |   |
| Rb     | 8.4                    | 15   | 16   | 18   | 17   | 16   | 15                   | 4.9  | ~3    | 22   | 14   | 6.6   | 3.2                    |   |   |   |   |   |
| Cs     | 0.31                   | 0.51 | 0.59 | 0.38 | 0.38 | 0.33 | 0.42                 | 0.63 | 0.41  | 0.31 | 0.25 | ~0.1  | 0.17                   |   |   |   |   |   |
| Sr     | 161                    | 227  | 196  | 238  | 205  | 173  | 200                  | 136  | 61    | 25   | 176  | 760   | 1800                   |   |   |   |   |   |
| Ba     | 97                     | 229  | 172  | 169  | 162  | 236  | 178                  | 57   | 21    | 42   | 44   | 41    | ~15                    |   |   |   |   |   |
| Th     | 2.8                    | 2.8  | 2.8  | 2.9  | 2.7  | 2.8  | 2.8                  | 0.55 | 0.54  | 0.52 | 0.66 | 0.66  | 0.58                   |   |   |   |   |   |
| U      | 0.57                   | 0.51 | 0.57 | 0.61 | 0.54 | 0.56 | 0.56                 | 0.20 | 0.20  | 0.16 | 0.17 | 0.23  | 0.25                   |   |   |   |   |   |
| Zr     | 195                    | 202  | 207  | 191  | 178  | 189  | 194                  | 106  | 109   | 108  | 67   | 132   | 199                    |   |   |   |   |   |
| Y      | 15                     | 14   | 16   | 14   | 12   | 13   | 14                   | 25   | 27    | 35   | 12   | 7.2   | —                      |   |   |   |   |   |
| Nb     | 17                     | 15   | 13   | 13   | 11   | 13   | 14                   | 12   | 13    | 15   | 10   | 8     | 5.6                    |   |   |   |   |   |
| Hf     | 3.4                    | 3.3  | 3.2  | 3.2  | 3.0  | 3.3  | 3.2                  | 2.8  | 2.9   | 3.1  | 1.8  | 1.9   | 1.6                    |   |   |   |   |   |
| Ta     | 0.55                   | 0.54 | 0.45 | 0.52 | 0.49 | 0.49 | 0.51                 | 0.28 | 0.42  | 0.36 | 0.22 | 0.26  | 0.20                   |   |   |   |   |   |
| Br     | 0.12                   | —    | —    | 0.08 | 0.08 | —    | 0.09                 | 0.07 | —     | 0.06 | 0.06 | 0.13  | 0.15                   |   |   |   |   |   |
| La     | 15                     | 18   | 18   | 19   | 17   | 19   | 18                   | 5.7  | 6.3   | 6.8  | 3.7  | 4.2   | 3.6                    |   |   |   |   |   |
| Ce     | 43                     | 41   | 39   | 37   | 37   | 40   | 40                   | 14   | 15    | 17   | 11   | 10    | 10                     |   |   |   |   |   |
| Nd     | 21                     | 16   | 19   | 19   | 15   | 18   | 18                   | 9    | 12    | 13   | 8.0  | 7.2   | —                      |   |   |   |   |   |
| Sm     | 4.8                    | 4.6  | 4.5  | 4.4  | 4.4  | 4.4  | 4.5                  | 3.0  | 2.9   | 3.4  | 1.9  | 1.9   | 1.8                    |   |   |   |   |   |
| Eu     | 1.5                    | 1.6  | 1.3  | 1.4  | 1.4  | 1.5  | 1.5                  | 1.4  | 1.5   | 1.2  | 0.84 | 0.77  | 0.87                   |   |   |   |   |   |
| Tb     | 0.64                   | 0.67 | 0.66 | 0.57 | 0.60 | 0.63 | 0.63                 | 0.66 | 0.71  | 0.79 | 0.43 | 0.47  | 0.40                   |   |   |   |   |   |
| Yb     | 1.5                    | 1.7  | 1.7  | 1.6  | 1.4  | 1.5  | 1.6                  | 3.3  | 3.1   | 3.5  | 1.8  | 1.6   | 1.7                    |   |   |   |   |   |
| Lu     | 0.24                   | 0.25 | 0.25 | 0.23 | 0.23 | 0.23 | 0.24                 | 0.65 | 0.61  | 0.68 | 0.33 | 0.31  | 0.30                   |   |   |   |   |   |
| K/Rb   | 366                    | 426  | 343  | 503  | 566  | 545  | 470                  | 407  | ~277  | 320  | 350  | 755   | 493                    |   |   |   |   |   |
| Rb/Sr  | 0.05                   | 0.07 | 0.08 | 0.08 | 0.08 | 0.09 | 0.08                 | 0.04 | ~0.05 | 0.88 | 0.08 | 0.008 | 0.002                  |   |   |   |   |   |
| K/Ba   | 32                     | 28   | 32   | 54   | 59   | 37   | 40                   | 35   | 40    | 168  | 111  | 121   | 105                    |   |   |   |   |   |
| Th/U   | 4.9                    | 5.5  | 4.9  | 4.8  | 5.0  | 5.0  | 5.0                  | 2.8  | 2.7   | 3.3  | 3.9  | 2.9   | 2.3                    |   |   |   |   |   |
| La/Yb  | 10.0                   | 10.6 | 10.6 | 11.9 | 12.1 | 12.7 | 11.3                 | 1.7  | 2.0   | 1.9  | 2.1  | 2.6   | 2.1                    |   |   |   |   |   |
| Ba/Sr  | 0.60                   | 1.0  | 0.88 | 0.71 | 0.79 | 1.4  | 0.89                 | 0.45 | 0.35  | 1.7  | 0.25 | 0.05  | 0.008                  |   |   |   |   |   |
| Zr/Nb  | 12                     | 14   | 16   | 15   | 16   | 14   | 15                   | 8.8  | 8.4   | 7.2  | 6.7  | 17    | 36                     |   |   |   |   |   |
| Eu/Eu* | 1.0                    | 1.1  | 0.90 | 1.0  | 1.0  | 1.1  | 1.0                  | 1.3  | 1.4   | 0.96 | 1.2  | 1.1   | 1.3                    |   |   |   |   |   |

\* Concentrations in ppm except Au which is ppb; dash indicates below level of detectability

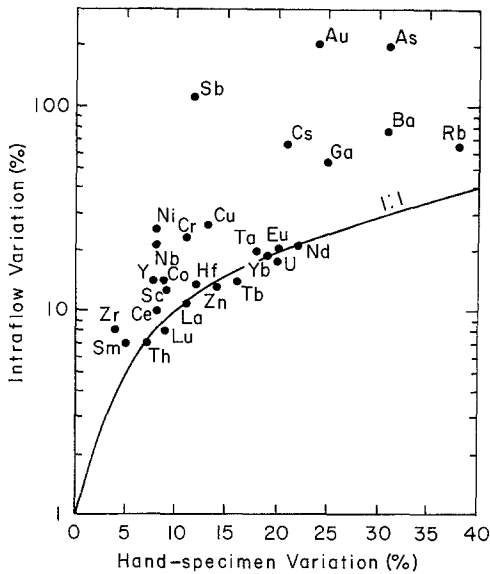


**Fig. 1.** Comparison of hand specimen (sample 22) and intraflow chemical variation in the LR flow. Variation = range  $\times$  100/mean

correlation exists between K and the three element ratios. Unless low-grade metamorphism completely obliterated the chemical signatures characteristic of low-temperature alteration, it would appear that the LR flow was not subjected to such alteration.

In order to evaluate possible effects of low-grade metamorphism on geochemistry, it is interesting to compare element variation in the LR flow with a modern unaltered tholeiite flow. Such a comparison is made in Figure 3 where element (and element ratio) variations in the Callahan flow of Recent age from the Medicine Lake area in northern California (Condie and Hayslip, 1975) are plotted as a function of corresponding variations in the LR flow. The Callahan flow is a typical subareal, calc-alkaline tholeiite flow and shows no signs of alteration. The fact that most elements (including the range in REE distributions, Fig. 2a) exhibit approximately the same amount of variability in both flows is consistent with the possibility that lowgrade metamorphism has not seriously modified element distributions in the LR flow. Exceptions are K, Rb, Sr, Na, and Nd which are more variable in the LR than in the Callahan flow. The greater variation in K, Rb, Sr, and Na in the LR flow is not surprising in that these elements are readily mobilized during both alteration and low-grade metamorphism. The greater variation in Nd in the LR flow probably reflects greater analytical error in the INNA method than in the RNNa method, the latter of which was used in analyzing the Callahan flow.

Element variability in the carbonated (CA) and epidotized (EP) flows are compared to that in the unaltered LR flow in Figure 4. The element variabilities in each flow are recalculated to 100% and plotted on a triangular graph in this figure. The corresponding variation of REE patterns within the CA and EP flows is shown in Figure 2b. The elements in group I (Fig. 4) (including

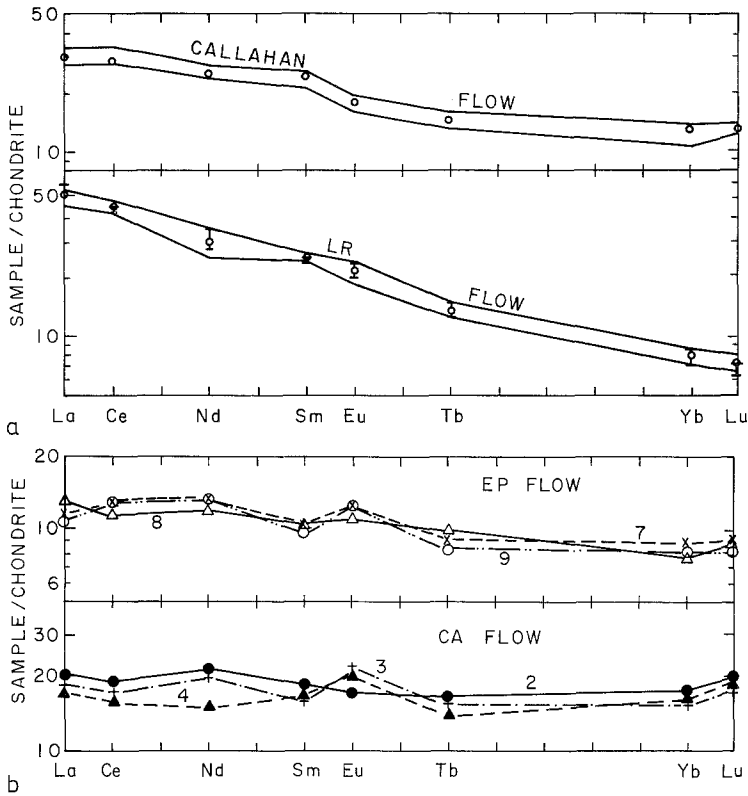


Fig. 2a and b. Chondrite-normalized REE distributions. a Envelopes of variation for LR and Callahan flows; circles represent mean values and vertical bars are the ranges of variation in hand specimen 22. b EP and CA flows, sample numbers correspond to those in Table 1

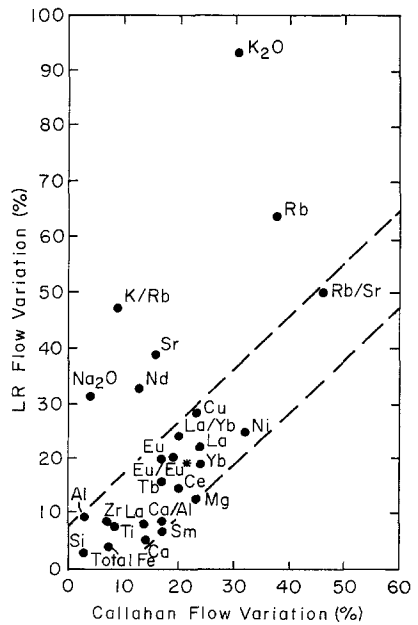


Fig. 3. Comparison of intraflow element variation in the LR and Callahan flows. Variation defined as in Figure 1; Callahan flow represents 7 samples

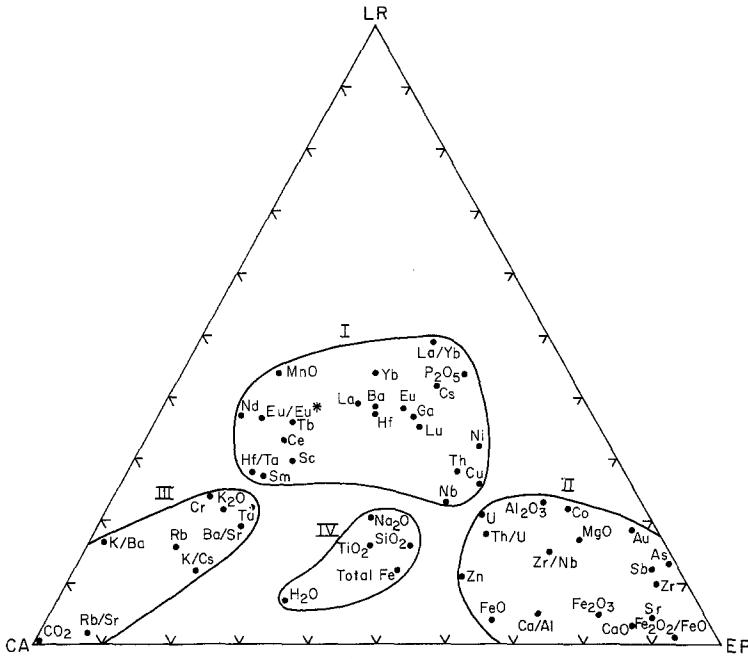


Fig. 4. Comparison of intraflow chemical variation in LR (unaltered), CA (carbonated), and EP (epidotized) flows. Range of variation in LR flow defined in Figure 1; range of variation in EP and CA = maximum deviation from value of unaltered sample  $\times 100$ /unaltered sample value

Hf, Ba, Ga, and REE) have approximately the same variabilities in the altered flows as in the unaltered flow and hence, do not appear to have been greatly modified by the alteration processes. It is these elements that should be given most weight in characterizing original magmas and in studying their origin. Elements in group II are mobilized by epidotization, those in group III by carbonization (+ chloritization), and those in group IV by both alteration processes. It is noteworthy that the alkali elements are mobilized by carbonization but not epidotization and that the opposite is true for Au, Sb, As, and Sr. The small variation in Cs (in group I) is somewhat surprising in that studies of low-temperature alteration (Hart, 1969) indicate that Cs is among the most mobile elements. Perhaps Cs is so mobile that a rather uniform distribution is attained over a large volume of rock during incipient alteration and such a distribution is not effected by later more intense alteration.

### Epidotization

Changes in element concentration with increasing amount of epidotization (Table 1, samples 7 to 9) are summarized in Tables 1 and 2 and in Figure 5. Most of the major-element changes and some of the trace element changes can be related to changes in modal mineralogy (Table 1). For instance, increases in



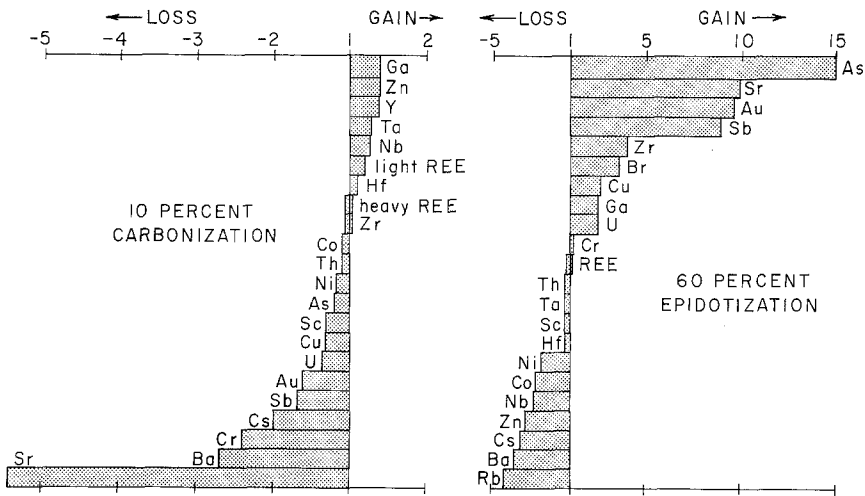


Fig. 5. Summary of losses and gains of trace elements accompanying carbonization and epidotization of Barberton tholeiites

$\text{Fe}^{+3}$  and Ca and decreases in  $\text{Fe}^{+2}$ , Mg, Si, and  $\text{H}_2\text{O}$  reflect increases in the amount of epidote at the expense of actinolite and plagioclase. On the  $\text{MgO-CaO-Al}_2\text{O}_3$  diagrams suggested by Viljoen and Viljoen (1969b) to identify Barberton komatiites, progressive epidotization results in increases in CaO and Ca/Al. On an  $\text{Al}_2\text{O}_3\text{-FeO}^*/\text{FeO}^* + \text{MgO}$  diagram, which was suggested by Naldrett and Cabri (1976) as a more general means of defining komatiites (except those from Barberton), sample 7 falls in the komatiite field and progressive epidotization of samples 7 to 9 moves compositions into the tholeiite-picrite field by increasing the  $\text{FeO}^*/\text{FeO}^* + \text{MgO}$  ratio. Almost all of the  $\text{TiO}_2$  in the EP rocks must reside in modal sphene which decreases slightly (as does  $\text{TiO}_2$ ) with epidotization. The abrupt drop in K, Na, and Ba between samples 8 and 9 seems to reflect the corresponding decrease in plagioclase. Rb also is lost during epidotization. The very large increase in Sr and more moderate increases in Ga and Br with epidotization suggest that these elements are housed in epidote. Melson et al. (1968) also observed an increase in Sr with epidotization of modern rise tholeiites. Au, Sb, and As increase by an order of magnitude in going from samples 7 to 9. Cu also shows a small increase but Zn decreases over this interval. Irregularly distributed sulfides which house some or perhaps all of these elements, also increase in abundance with epidotization. Clearly, some chalcophile elements and Au were introduced during epidotization. The relatively small changes in U and Cs contents with epidotization are surprising considering the documented mobilities of these elements (Hart, 1969; Aumento, 1971). As mentioned above for Cs in the LR flow, it is possible that a uniform distribution of these elements was reached during an early stage of alteration and not significantly changed thereafter. The moderate decreases in Co and Ni and small decrease in Sc with epidotization parallel decreases in actinolite and iron oxides which probably host these elements. It is noteworthy that

Zr increases and Nb decreases during epidotization leading to a significant increase in the Zr/Nb ratio. Hence, when using epidotized basalts, care should be taken in deducing the presence or absence of undepleted mantle based on this ratio as suggested by Erlank and Kable (1976). With exception of the magnitude of the Eu anomaly which varies non-systematically with epidotization (Fig. 2b), REE patterns are not appreciably affected up to about 60% epidotization. Together with the REE, Hf, Ta, Sc, Cr, and Th concentrations are least affected by progressive epidotization (Fig. 5).

### Carbonization

Changes in composition accompanying carbonization-chloritization are also summarized in Tables 1 and 2 and in Figure 5. The increase in  $\text{CO}_2$  parallels the increase in modal carbonate in samples 4 to 2 and the increase in  $\text{Fe}^{+2}$  and  $\text{H}_2\text{O}$  and decrease in Ca and Si reflect primarily the increasing amounts of chlorite and iron oxides in this sequence. It is noteworthy that Ca is lost during carbonization. The drop in Na in going from samples 3 to 2 reflects a decrease in plagioclase and the corresponding increase in K is probably controlled by an abrupt increase in the amount of sericite (the probable host mineral). Effects of carbonization-chloritization on samples when plotted in the  $\text{CaO}-\text{MgO}-\text{Al}_2\text{O}_3$  diagram are to decrease Ca and the Ca/Al ratio. On the  $\text{Al}_2\text{O}_3-\text{FeO}^*/\text{FeO}^*+\text{MgO}$  diagram,  $\text{Al}_2\text{O}_3$  decreases slightly but all samples remain in the tholeiiticpicrite field.  $\text{TiO}_2$  increases with carbonization. It is clear from these results that carbonization-chloritization can modify bulk composition in such a way that original basaltic komatiites could change into rocks with tholeiite characteristics (employing the definitional parameters of Brooks and Hart, 1974). As with K, the abrupt increase in Rb, K/Rb, K/Ba, and K/Cs between samples 3 and 2 parallels and probably reflects the increase in sericite. Cs is an exception among the alkali elements showing a moderate decrease with carbonization. Sr and Ba follow Ca, decreasing with carbonization. K/Cs, and less pronounced K/Rb, decrease with K a feature characteristic of low-temperature alteration. On the whole, depletion in Ca, Mn, and Au (and to a smaller extent Ni, Co, and Sc) parallel decreasing actinolite and increasing iron oxide phases. Perhaps the most striking feature of the REE patterns is their similarity in both the unaltered and carbonated samples (Fig. 2b). Light REE are, however, slightly enriched in the two carbonated samples and sample 2 has a low Eu content paralleled by a decrease in plagioclase. Although containing a factor of two more REE, the REE patterns in the CA flow are similar to those in the EP flow. Hf, Ni, Co, Th, Zr, and heavy REE are most resistant to change during small amounts of carbonization (Fig. 5).

### Model Studies

Because geochemical investigations of the origin of greenstone magmas rely on the assumption that alteration has not significantly modified element distribution (Condie and Harrison, 1976; Condie, 1976), it is of interest to examine

the effects of alteration as documented in this study on magma production models. The approach, which involves both major and trace elements is described in Condie and Harrison (1976) and Condie and Hunter (1976). Only the unaltered samples (4 and 7) were used in the major-element calculations for the EP and CA flows. Trace elements employed are those least susceptible to mobilization for which distribution coefficient data are available. Models tested involve both fractional crystallization and partial melting as summarized in Table 3. Unless otherwise specified, distribution coefficients are from Condie and Harrison (1976).

In the classification of Archean volcanic rocks suggested by Condie (1976), the LR flow is most accurately identified as EAT. Its  $Al_2O_3$ - $FeO^*/FeO^* + MgO$  relations and high Cr, Co, and Ni, however, suggest that it is an alkali-rich basaltic komatiite (similar to the Barberton-type). Clearly it has komatiitic affinities. Crystallization and melting models for the LR flow not involving garnet as a residual phase are unacceptable in that fractionated REE patterns cannot readily be produced. Even a garnet peridotite source cannot produce a melt with a high enough light REE content without going to <20% melting which is not allowed by other elements. Major-elements give poor internal agreement for all ultramafic melting models. Of the mafic-parent melting models, eclogite results in the best overall match for most elements. Amphibolite and gabbro cannot produce fractionated enough REE patterns and garnet granulite and garnet amphibolite produce magmas too low in Sr. If Sr were significantly enriched in the LR flow by alteration (evidence for which is nonexistent), however, these latter two rock types would also have to be considered as possible parental materials.

**Table 3.** Summary of magma generation models tested<sup>a</sup>

| Process                    |              | Parent compositions tested |           |
|----------------------------|--------------|----------------------------|-----------|
| Fractional crystallization | Shallow      | } GP, PK                   |           |
|                            | Intermediate |                            |           |
|                            | Deep         |                            |           |
| Partial melting            | } Mafic      | Eclogite                   | } DAT, BK |
|                            |              | Garnet Granulite           |           |
|                            |              | Garnet Amphibolite         |           |
|                            |              | Amphibolite                |           |
|                            |              | Gabbro                     |           |
|                            | } Ultramafic | Lherzolite                 | } GP, PK  |
| Garnet Lherzolite          |              |                            |           |
| Plagioclase Lherzolite     |              |                            |           |

<sup>a</sup> GP=average garnet peridotite compiled by senior author (Condie and Harrison, 1976); PK=peridotitic komatiite and BK=basaltic komatiite, Barberton-type (Viljoen and Viljoen, 1969b; Hermann et al., 1976); DAT=depleted Archean tholeiite (Condie, 1976). Liquidus phases for crystallization models are given in Condie and Hayslip (1975)

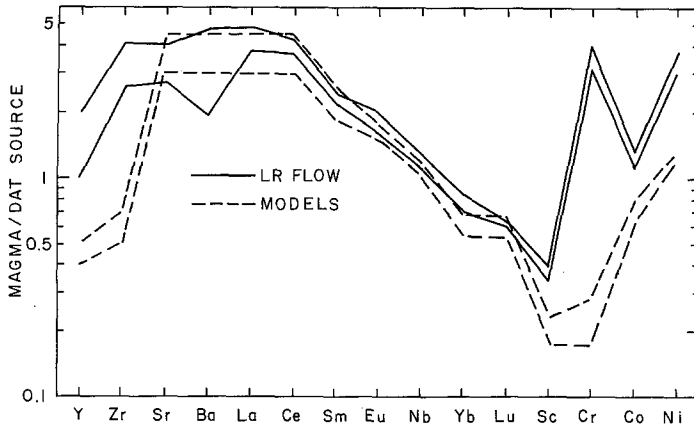


Fig. 6. Range of DAT-normalized trace element distributions in the LR flow compared to envelope of variation of eclogite melting models. Range of variables in models: cpx:gar ratio in residue 4:6 to 6:4; fraction of melting 0.2–0.3; Garnet REE distribution coefficients at 30 kb (Shimizu and Kushiro, 1975)

The range of variation of calculated eclogite models is compared to the range of trace-element variation in the LR flow in Figure 6 normalized to a DAT parent which gives slightly better results than a basaltic komatiite parent. Each is shown as an envelope of maximum variation. Variable parameters in the eclogite model are given in the Figure caption. With exception of Ba, the range of variation of the normalized LR flow is less than or approximately equal to that of the models. Clearly, the effect of element variation in the flow is negligible in terms of permitted model variation. One major problem with the eclogite model (and with most other models) is the high transition-metal and Y and Zr contents of the LR flow. Two possible causes for these discrepancies between the model and observed element ratios are 1) distribution coefficients for these elements are considerable lower than those used in the calculations or 2) the source is enriched in these elements compared to DAT or basaltic komatiite. If low distribution coefficients for Co, Ni, and Cr are used for clinopyroxene from experimental results at high temperature ( $\sim 1400^{\circ}\text{C}$ ) (references in Drake, 1976) and garnet distribution coefficients are assumed to be in the same range, only Co can be brought into agreement. For this reason, the second possibility is preferred to account for these differences. For Y and Zr, however, unreasonably large concentrations are required in the eclogite source ( $\text{Zr} \approx 400$  ppm,  $\text{Y} \approx 30$  ppm) if agreement is to be attained. Hence, lower distribution coefficients for garnet ( $D^{\text{Zr}} \leq 0.5$ ;  $D^{\text{Y}} \approx 0.5$ ) and for Zr in clinopyroxene ( $D^{\text{Zr}} < 1$ ) are a preferred explanation for these observed differences.

Of the models tested for the EP and CA flows, fractional crystallization models give poor agreement or are not allowed by the major elements (using unaltered compositions only). Some olivine ( $\pm$  orthopyroxene) removal (25–35%), however, is required by the  $\text{Mg}/\text{Mg} + \text{Fe}$  ratio of the rocks which

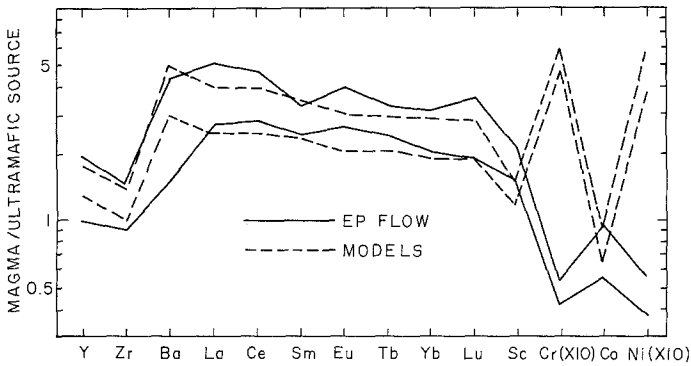


Fig. 7. Range of ultramafic-normalized trace element distributions in the EP flow compared to envelope of variation of lherzolite melting models. Parent-rock compositions range from average garnet peridotite (Condie and Harrison, 1976) to peridotitic komatiite (Hermann et al., 1976). Range of variables in models: fraction of melting 0.2–0.35; non-modal and modal melting of cpx-ol-opx-sp mixtures; high-pressure distribution coefficients for clinopyroxene when available (Shimizu, 1974); high-temperature ( $\sim 1400^\circ\text{C}$ ) distribution coefficients for Cr, Ni, and Co when available (summarized in Drake, 1976)

is not in equilibrium with mantle olivine ( $\text{Fo}_{90-92}$ ). Any melting model with residual garnet produces fractionated REE patterns in the melt a feature which is not observed in either flow. Amphibolite and gabbro parents give rise to melts depleted in REE and Sr compared to the CA and EP flows. Models with residual plagioclase give rise to both a negative Eu anomaly and Sr depletion in the melt, neither of which are observed. Partial melting of lherzolite results in the best agreement for production of the EP magma. The range of trace element variability caused by epidotization (using all EP samples) and uncertainties in source composition is shown as an envelope for the EP flow in Figure 7. Also shown is the envelope of variation for lherzolite melting models. Again, with exception of Ba, the variation of the envelopes is of the same magnitude indicating that for the trace elements used, epidotization does not significantly affect interpretation of the models. With exception of Ni and Co, removal of up to 35% olivine ( $\pm$  orthopyroxene) as mentioned above does not appreciably affect trace element patterns. If  $D_{01}^{\text{Ni}} \gtrsim 10$ , the observed discrepancy in Ni between the Ep flow and the model (Fig. 7) can be eliminated by such olivine removal. The poor agreement of Cr between sample and model envelopes is most easily explained by a residual Cr-spinel phase remaining in the source rock or also removed during fractional crystallization.

The CA flow differs primarily from the EP flow by its higher REE content. Five possible causes for this difference are as follows: 1) changes in bulk REE distribution coefficients due to differences in residual mineral proportions; 2) more extensive fractional crystallization of the CA flow; 3) smaller degree of melting of the source to produce the CA magma (5–10 percent); 4) all CA samples were enriched in REE during an earlier stage of alteration; and 5) the source for the CA magma was less depleted in REE than the source for the EP magma. Calculations indicate the effects of the first two causes are

negligible and major-element and other trace-element data will not allow  $\lesssim 20\%$  melting of the ultramafic source rock thus rendering cause 3 unlikely. Regarding cause 4, evidence was not found for alteration in sample 4 and if the REE patterns in all CA samples reflects alteration, a light-REE enriched pattern would be expected. The fifth cause is tentatively favored and is consistent with the plume model proposed by Condie and Hunter (1976) for the Barberton area. The CA flow would be derived from a relatively undepleted plume and the EP flow (later in the section) from perhaps the same plume source at a later time when it is partially depleted in REE. The results of this study verify earlier conclusions (Condie and Baragar, 1974; Condie and Hunter, 1976; Condie, 1976) that both mafic and ultramafic source rocks are necessary for greenstone magmas and that source rocks must be continually replenished.

*Acknowledgments.* We acknowledge the help of Pauline Richardson with the XRF analyses. REE analyses in the Callahan flow were done by M.J. Potts. The research was sponsored in part by NSF grant EAR76-11730 and a senior busary from the CSIR in South Africa both to the senior author. The research was done in the Department of Geology and the NPRU at the University of Witwatersrand while the senior author was on sabbatical leave. T.N. Clifford is thanked for his endless enthusiasm and hospitality during this period of time.

## References

- Aumento, F.: Uranium content of mid-oceanic basalts. *Earth Planet. Sci. Lett.* **11**, 90–94 (1971)
- Brooks, C., Hart, S.R.: On the significance of komatiite. *Geology* **2**, 107–110
- Condie, K.C.: Trace-element geochemistry of Archean greenstone belts. *Earth-Sci. Rev.* **12**, 393–417 (1976)
- Condie, K.C., Baragar, W.R.A.: Rare earth element distributions in volcanic rocks from Archean greenstone belts. *Contrib. Mineral. Petrol.* **45**, 237–246 (1974)
- Condie, K.C., Harrison, N.M.: Geochemistry of the Archean Bulawayan Group, Midlands greenstone belt, Rhodesia. *Precamb. Res.* **3**, 253–271 (1976)
- Condie, K.C., Hayslip, D.L.: Young bimodal volcanism at Medicine Lake volcanic center, northern California. *Geochim. Cosmochim. Acta* **39**, 1165–1178 (1975)
- Condie, K.C., Hunter, D.R.: Trace element geochemistry of Archean granitic rocks from the Barberton region, South Africa. *Earth Planet. Sci. Lett.* **20**, 389–400 (1976)
- Drake, M.J.: Evolution of major mineral compositions and trace element abundances during fractional crystallization of a model lunar composition. *Geochim. Cosmochim. Acta* **40**, 401–411 (1976)
- Erlank, A.J., Kable, E.J.D.: The significance of incompatible elements in Mid-Atlantic Ridge basalts from 45° N with particular reference to Zr/Nb. *Contrib. Mineral. Petrol.* **54**, 281–291 (1976)
- Frey, F.A., Bryan, W.B., Thompson, G.: Atlantic Ocean floor: geochemistry and petrology of basalts from Legs 2 and 3 of the Deep-Sea Drilling Project. *J. Geophys. Res.* **79**, 5507–5527 (1974)
- Hart, S.R.: K, Rb, Cs contents and K/Rb, K/Cs ratios of fresh and altered submarine basalts. *Earth Planet. Sci. Lett.* **6**, 295–303 (1969)
- Hart, S.R., Erlank, A.J., Kable, E.J.D.: Sea floor basalt alteration: some chemical and Sr isotope effects. *Contrib. Mineral. Petrol.* **44**, 219–230 (1974)
- Hermann, A.G., Blanchard, D.P.: Haskin, L.A., Jacobs, J.W., Knake, D., Korotev, R.L., Brannon, J.C.: Major, minor, and trace element compositions of peridotitic and basaltic komatiites from the precambrian crust of southern Africa. *Contrib. Mineral. Petrol.* **59**, 1–12 (1976)
- Melson, W.G., Thompson, G., Van Andel, T.H.: Volcanism and metamorphism in the Mid-Atlantic Ridge, 22° N Latitude. *J. Geophys. Res.* **73**, 5925–5941 (1968)

- Naldrett, A.J., Cabri, L.J.: Ultramafic and related mafic rocks: their classification and genesis with special reference to the concentration of nickel sulfides and platinum-group elements. *Econ. Geol.* **71**, 1131–1158 (1976)
- Norrish, K., Hutton, J.T.: An accurate X-ray spectrographic method for the analysis of a wide range of geological samples. *Geochim. Cosmochim. Acta* **33**, 431–453 (1969)
- Rasmussen, S.E., Fesq, H.W.: Neutron activation analysis of samples from the Kimberley Reef Conglomerate. Nat. Institute Metallurgy Rept. No. 1563 (1973)
- Scott, R.B., Hajash, Jr., A.: Initial submarine alteration of basaltic pillow lavas: a microprobe study. *Am. J. Sci.* **276**, 480–501 (1976)
- Shapiro, L., Brannock, W.W.: Rapid analysis of silicate rocks. U.S. Geol. Surv. Bull. 1036-C (1956)
- Shimizu, N.: An experimental study of the partitioning of K, Rb, Cs, Sr and Ba between clinopyroxene and liquid at high pressures. *Geochim. Cosmochim. Acta* **38**, 1789–1798 (1974)
- Shimizu, N., Kushiro, I.: the partitioning of rare earth elements between garnet and liquid at high pressures: preliminary experiments. *Geophys. Res. Lett.* **2**, 413–416 (1975)
- Steinnes, E.: Epithermal neutron activation analysis of geological material. In: *Activation analysis in geochemistry and cosmochemistry* (A.O. Brunfelt and E. Steinnes, eds.), pp. 113–128. : Universitetsforlaget 1971
- Viljoen, J.J., Viljoen, R.P.: The geologic and geochemical significance of the upper formations of the Onverwacht Group. *Geol. Soc. South Afr. Spec. Publ. No. 2*, 113–154 (1969c)
- Viljoen, M.J., Viljoen, R.P.: The geology and geochemistry of the lower ultramafic unit of the Onverwacht Group and a proposed new class of igneous rock. *Geol. Soc. South Afr. Spec. Publ. No. 2*, 55–86 (1969b)
- Viljoen, R.P., Viljoen, M.J.: The effects of metamorphism and serpentization on the volcanic and associated rocks of the Barberton region. *Geol. Soc. South Afr. Spec. Publ. No. 2*, 29–54 (1969a)
- Wood, D.A., Gibson, I.L., Thompson, R.N.: Elemental mobility during zeolite facies metamorphism of the Tertiary basalts of eastern Iceland. *Contrib. Mineral. Petrol.* **55**, 241–254 (1976)

*Received May 3, 1977 | Accepted June 2, 1977*